Materials and Methods

Aorta intima RNA isolation

Aorta intimal RNA was obtained as previously described [2]. Briefly, mouse aortas were exposed, and the surrounding tissues were removed carefully. After perfusion with saline, the aorta was collected and transferred to a dish containing ice-cold PBS. To obtain samples from predilection sites and nonpredilection sites, the aorta was cut into two parts: the aortic arch (predilection sites) and the thoracoabdominal aorta (nonpredilection sites). The preparation was quickly flushed with TRIzol reagent (Invitrogen, Carlsbad, CA, USA) using an insulin syringe, and the eluate was collected in a 1.5-ml tube and prepared for RNA extraction. The aorta leftover (media +adventitia) was stored at -80℃ until RNA extraction.

RNA Sequencing

Total RNA from pre-treated HAECs was extracted by using Trizol regent, and purified with RNAClean XP Kit (Cat A63987, Beckman Coulter, Inc. Kraemer Boulevard Brea, CA, USA) and RNase-Free DNase Set (Cat#79254, QIAGEN, GmBH, Germany). The purity and integrity of total RNA samples were determined using the Agilent Bioanalyzer (Agilent Technologies, Santa Clara, CA, USA). Next, samples were treated with RiboZero rRNA Removal Kit (Epicentre, WI, USA) for deleting rRNA. Then, rRNA-depleted and RNase R-digested RNA samples were fragmented, and reverse transcribed to cDNAs with random primers. After purification, cDNA libraries were quality controlled and sequenced by HiSeq2000 (Illumina, San Diego, CA, USA).

Sequence Data Analysis

Raw reads in fastq format were screened, and the adaptor sequences and low-quality reads were deleted. Stringent filtering criteria were selected to diminish the ratio of sequencing errors. Briefly, bases with a 3 terminal quality score lower than 10 and a read-length shorter than 20 bp were removed. Genome mapping was performed based on the E. necatrix Houghton strain reference genome sequence (GCA_000499385.1) using Tophat (version 2.0.9) with a spliced-mapping algorithm. After genome mapping, reads with less than two-base mismatches and multi hits$\leq$ 2 were retained.

Result

lncR-GAS5 transfection efficacy and atherosclerotic model

To investigate the role of lncR-GAS5 in atherogenesis, 8-week-old athero-prone *ApoE*$^{-/-}$ mice fed with a high-fat diet (HFD) were intravenously injected with recombinant lentivirus vector-expressing lncR-GAS5 (Lv-GAS5), empty vector (Lv-null) as a negative control, equal volume of saline fed with a HFD or a chow diet (CD) as normal for 12 weeks (Supplementary Fig. 1A). As shown in supplementary Fig. 1B, mRNA expression of the endothelial cells (ECs) marker CD31 was enriched in the intima compared with media plus adventitia. Conversely, the smooth muscle cell marker smMHC was rarely detectable in the intima, manifesting high purity ECs were obtained from aortic intima (Supplementary Fig. 1C). Notably, compared with the intima, the lncR-GAS5 expression was lower in the media plus adventitia, indicating that lncR-GAS5 is more abundant in ECs (Supplementary Fig. 1D). We also observed that lncR-GAS5 was dominantly increased in ECs of *ApoE*$^{-/-}$ mice fed with HFD (Supplementary Fig. 1E). Our result indicated that lncR-GAS5 overexpression repressed the mRNA level of MAP1LC3B and increased the P62 expression in endothelium of en face aortas (Supplementary Fig. 1F and 1G).

lncR-GAS5 potentiates mice to develop abnormal hyperlipidemia, but not Alters body weight (BW), Blood pressure, Glucose metabolism

We next collected blood samples by retro-orbital venous plexus puncture to assess the alteration of circulating metabolic parameters after mice were fasted for 12–14 h. Result indicated that lncR-GAS5 overexpression markedly elevated expression of total cholesterol (TC), triglycerides (TG), low-density lipoprotein cholesterol (LDL-C), and reduced the level of high-density lipoprotein cholesterol (HDL-C) under fasting conditions, respectively (Supplementary Fig. 2A, 2B, 2C and 2D). Next, Body weight (BW) was further measured weekly during 12 weeks in mice fed with HFD. Result indicated that even Lv-GAS5 treatment could increase BW in a time dependent manner, while showed no statistically significant (Supplementary Fig. 2E). Abnormal of blood pressure and blood glucose are one of the leading causes of atherosclerosis. It is documented that high level of lncR-GAS5 had no influence on systolic blood pressure (SBP, mmHg) in mice fed chow diet (CD) or HFD

(Supplementary Fig. 2F). Insulin sensitivity decrease or insulin resistant is one of the main reasons of atherogenesis [1, 3]. Our result showed that Lv-GAS5 upregulation had little influenced on insulin sensitivity and glucose homeostasis during an insulin tolerance test (ITT) and glucose tolerance tests (GTT), respectively (Supplementary Fig. 2G and 2H).

lncR-GAS5 associated regulator was screened

To gain insight into the molecular mechanism by which lncR-GAS5 regulates autophagy, we performed tailored RNA sequencing (RNA-seq). After cells were transfected with small interfering RNA against lncR-GAS5 for 24 h, the cells were collected for analysis using RNA-seq. Gene ontology analysis indicated that lncR-GAS5 knockdown resulted in the upregulation of 305 genes and downregulation of 138 genes based on the criterion of a ≥2-fold change in expression, and these differentially expressed genes have been implicated in biological regulation, cellular processes, , metabolic processes, and molecular function regulation (Supplementary Fig. 3A). Volcano plots show the distribution of these differentially expressed genes (Supplementary Fig. 3B). KEGG pathway enrichment analyses showed that the differentially expressed genes are associated with immune systerm, lipid metabolism and signal transduction (Supplementary Fig. 3C).

Figure legend

Fig. S1. Detection of lncR-GAS5 lentivirus infective efficacy and its effects on MAP1LC3B and P62 expression in HFD-fed *ApoE*$^{-/-}$ mice. (A) Experiment procedure. (B-D) The expression levels of CD31 (B), smMHC (C), and lncR-GAS5 in HFD-fed *ApoE*$^{-/-}$ mice. n=4 male *ApoE*$^{-/-}$ mice. (E) The expression levels of lncR-GAS5 in *ApoE*$^{-/-}$ with HFD or CD. n=5 male *ApoE*$^{-/-}$ mice. (F and G) The effect of lncR-GAS5 on the expression of MAP1LC3B (F) and P62 (G) in HFD-fed *ApoE*$^{-/-}$ mice. $^{**}P$ <0.01 vs. Intima or CD or Lv-null group. All values are expressed as the mean ± SEM.

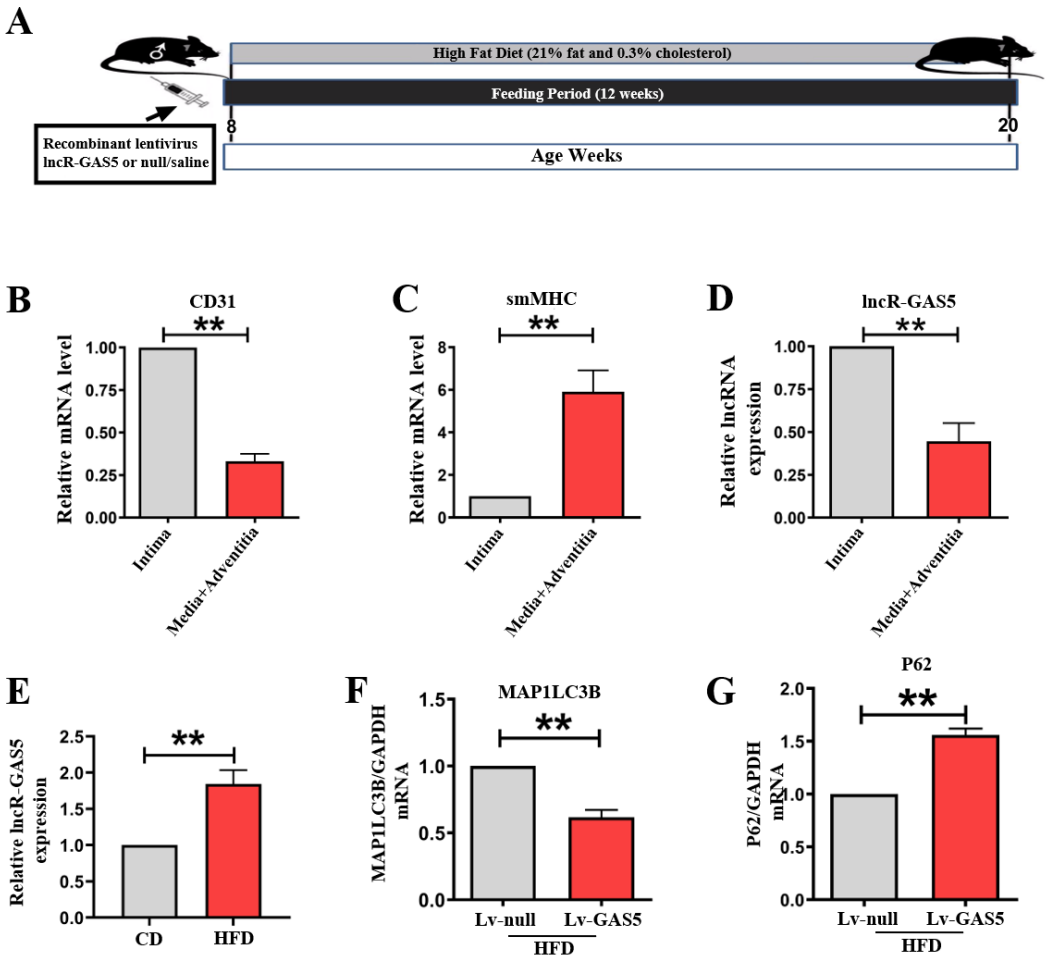

92

93 **Fig. S2. Fig. S2. The effect of lncR-GAS5 overexpression on lipid and lipid**
94 **protein expression, systolic blood pressure (SBP), and blood glucose in HFD-fed**
95 ***ApoE*$^{-/-}$ mice.** (A-D) The expression levels of TC (A), TG (B), LDL-C (C), and
96 HDL-C (D). (E) The body weight of mice. (F) The effect of lncR-GAS5
97 overexpression on SBP of HFD-fed *ApoE*$^{-/-}$ mice. (G and H) The effect of lncR-GAS5
98 overexpression on ITT (G) and GTT (H) of HFD-fed *ApoE*$^{-/-}$ mice. "+" indicated mice
99 fed with HFD. n=8 male *ApoE*$^{-/-}$ mice. *$p < 0.05$, **$p < 0.01$ vs. Lv-null+ group. All
100 data represent the mean ±S.E.M.

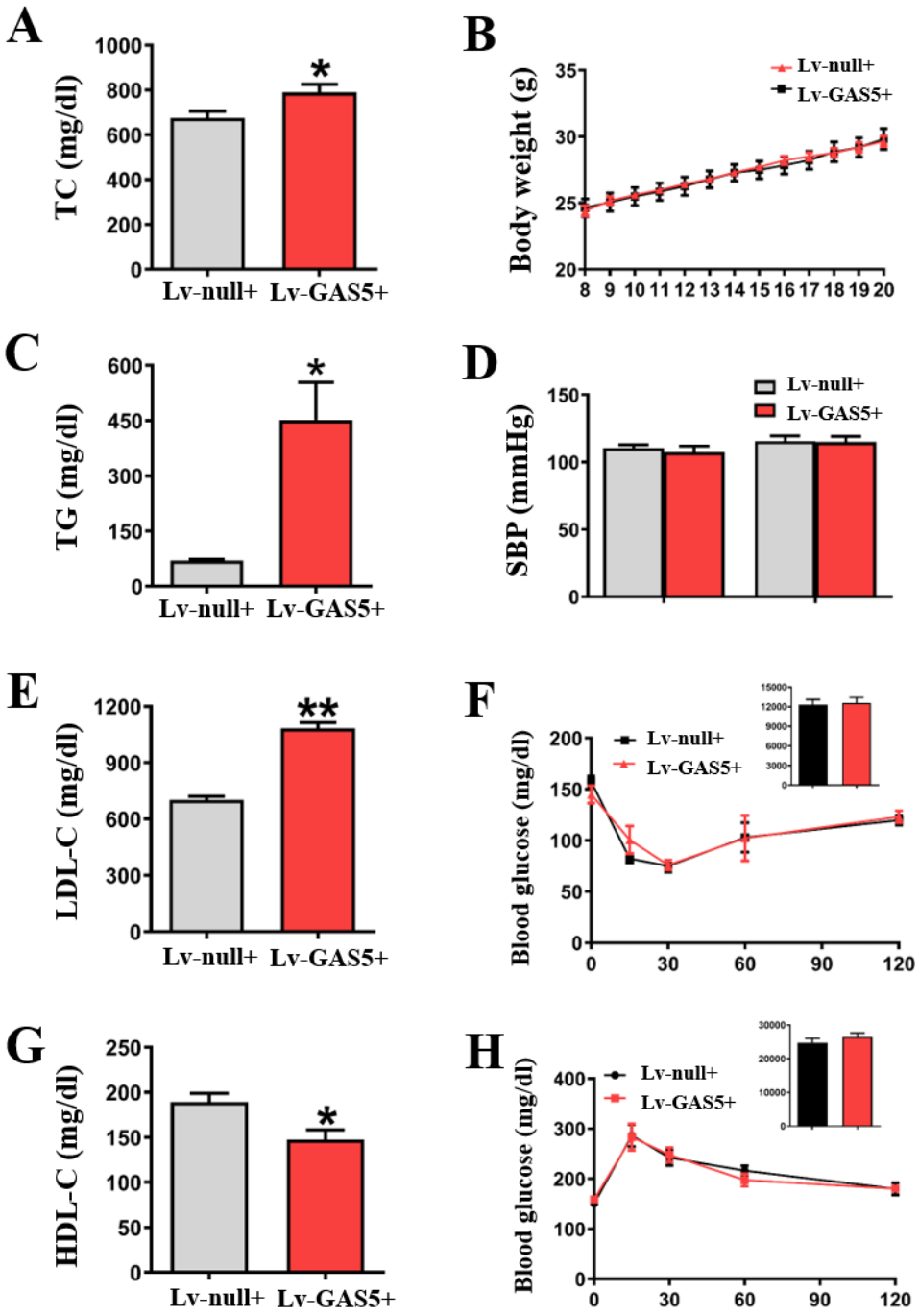

Fig. S3. Fig. S3. GO and KEGG enrichment analysis of differentially expressed genes after lncR-GAS5 knockdown. (A) GO enrichment analysis of the differentially expressed genes after lncR-GAS5 knockdown. (B) The distribution of differentially expressed genes after lncR-GAS5 knockdown. (C) KEGG enrichment analysis differentially expressed genes after lncR-GAS5 knockdown. n=3 batches of cells.

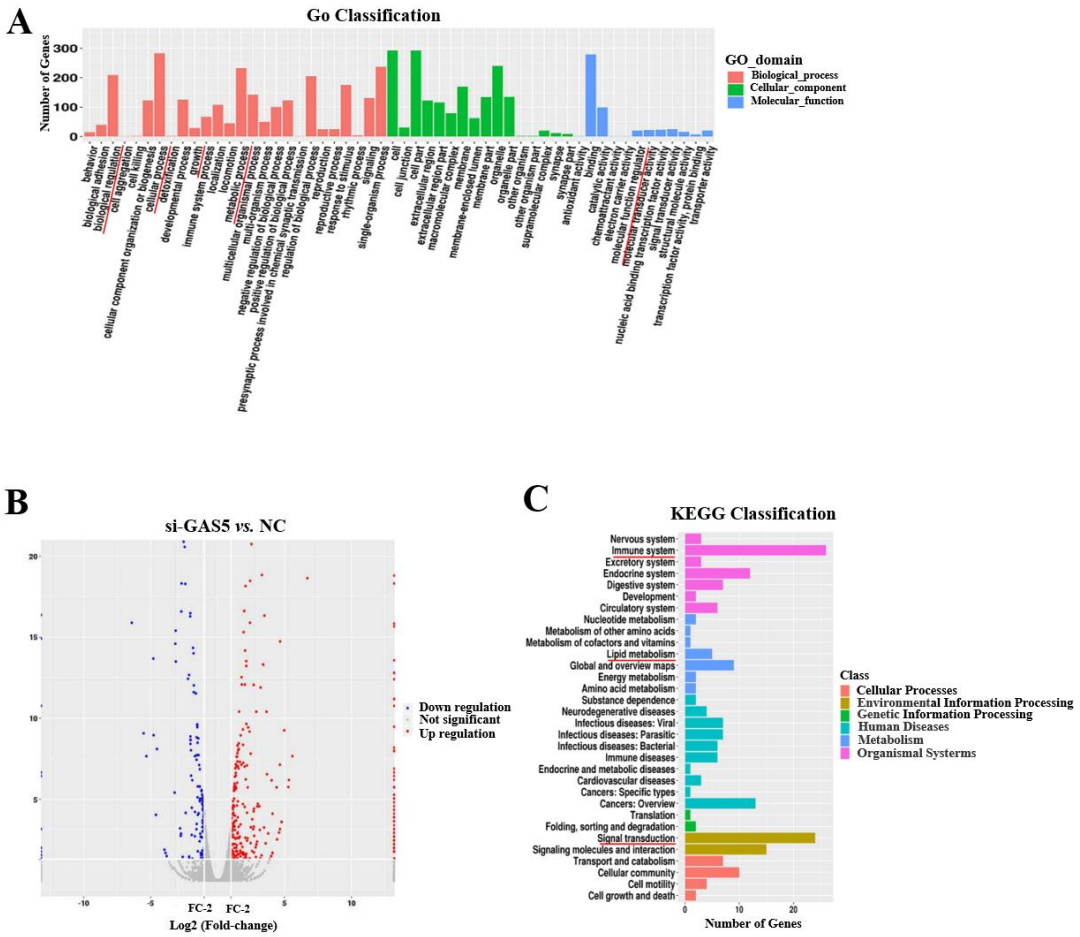

References

1. Martinez-Hervas S, Vinue A, Nunez L, Andres-Blasco I, Piqueras L, Real JT, Ascaso JF, Burks DJ, Sanz MJ, Gonzalez-Navarro H (2014) Insulin resistance aggravates atherosclerosis by reducing vascular smooth muscle cell survival and increasing CX3CL1/CX3CR1 axis. Cardiovascular research 103:324-336 doi:10.1093/cvr/cvu115
2. Sun X, He S, Wara AKM, Icli B, Shvartz E, Tesmenitsky Y, Belkin N, Li D, Blackwell TS, Sukhova GK, Croce K, Feinberg MW (2014) Systemic delivery of microRNA-181b inhibits nuclear factor-kappaB activation, vascular inflammation, and atherosclerosis in apolipoprotein E-deficient mice. Circulation research 114:32-40 doi:10.1161/CIRCRESAHA.113.302089
3. Yongming P, Zhaowei C, Yichao M, Keyan Z, Liang C, Fangming C, Xiaoping X, Quanxin M, Minli C (2015) Involvement of peroxisome proliferator-activated receptors in cardiac and vascular remodeling in a novel minipig model of insulin resistance and atherosclerosis induced by consumption of a high-fat/cholesterol diet. Cardiovasc Diabetol 14:6 doi:10.1186/s12933-014-0165-0